

Morphing Graph Drawings in the Presence of Point Obstacles[★]

Oksana Firman^a, Tim Hegemann^a, Boris Klemz^{a,*}, Felix Klesen^a, Marie Diana Sieper^a, Alexander Wolff^a and Johannes Zink^a

^aInstitut für Informatik, Universität Würzburg, Würzburg, Germany

ARTICLE INFO

Keywords:

Graph morphing
Point obstacles
NP-hard
Planar graph

ABSTRACT

A crossing-free morph is a continuous deformation between two graph drawings that preserves straight-line pairwise noncrossing edges. Motivated by applications in 3D morphing problems, we initiate the study of morphing graph drawings in the plane in the presence of stationary point obstacles, which need to be avoided throughout the deformation.

As our main result, we prove that it is NP-hard to decide whether such an obstacle-avoiding 2D morph between two given drawings of the same graph exists. In fact, this statement remains true even in the severely restricted special case where only three vertices have to change positions. This is in sharp contrast to the classical case without obstacles, where there is an efficiently verifiable (necessary and sufficient) criterion for the existence of a morph.

Further, we provide several combinatorial results related to conditions under which the existence of a morph between two drawings of a graph can or cannot be prevented by the placement of a given number of point obstacles.

1. Introduction

In the field of Graph Drawing, a *morph* between two straight-line drawings Γ_1 and Γ_2 of the same graph is a continuous deformation that transforms Γ_1 into Γ_2 while preserving straight-line edges at all times. A morph is *crossing-free*¹ if the edges are pairwise noncrossing at all times. Morphing (beyond the above, strict definition in Graph Drawing) has applications in animation and computer graphics [14]. In this paper, we initiate the study of morphing graph drawings in the presence of stationary point obstacles, which need to be avoided throughout the motion.

Related work. An obvious necessary condition for the existence of a crossing-free morph in \mathbb{R}^2 between two straight-line drawings Γ_1 and Γ_2 is that these drawings represent the same *plane graph* (i.e., a planar graph equipped with fixed combinatorial embedding and a distinguished outer face). It has been established long ago [8, 19] that this (efficiently verifiable) criterion is also sufficient, i.e., a crossing-free morph in \mathbb{R}^2 between two straight-line drawings of the same plane graph always *exists*.

More recent work [2, 16] focuses on efficient *computation* of such morphs. In particular, this involves producing a discrete description of the continuous motion. Typically, this is done in form of so-called piecewise linear morphs. In a *linear* morph, each vertex moves along a straight-line segment at a constant speed (which depends on the length of the segment) such that it arrives at its final destination at the end of the morph. The (unique) linear morph between Γ_1 and Γ_2 is denoted by $\langle \Gamma_1, \Gamma_2 \rangle$. A *piecewise linear* morph is created by concatenating several linear morphs, which are referred to as (*morphing*) *steps*. A piecewise linear morph consisting of k steps can be encoded as a sequence of $k + 1$ drawings. Alamdari et al. [2] showed that two straight-line drawings of the same n -vertex plane graph always admit a crossing-free piecewise linear morph in \mathbb{R}^2 with $O(n)$ steps, which is best-possible. Their proof is constructive and corresponds to an $O(n^3)$ -time algorithm, which was later sped up to $O(n^2 \log n)$ time by Klemz [16].

[★]Work partially supported by DFG grants WO 758/9-1 and WO 758/11-1. A preliminary version of this article appeared in the proceedings of SOFSEM 2024 [13].

*Corresponding Author

✉ `firstname.lastname@uni-wuerzburg.de`

ORCID(s): 0000-0002-9450-7640 (O. Firman); 0009-0008-4770-3391 (T. Hegemann); 0000-0002-4532-3765 (B. Klemz); 0000-0003-1136-5673 (F. Klesen); 0009-0003-7491-2811 (M.D. Sieper); 0000-0001-5872-718X (A. Wolff); 0000-0002-7398-718X (J. Zink)

¹In the context of morphs restricted to the plane \mathbb{R}^2 , crossing-free morphs are usually called *planar*. Since we are also discussing work related to morphs in three dimensions, we are using the more general term crossing-free in the beginning of our introduction.

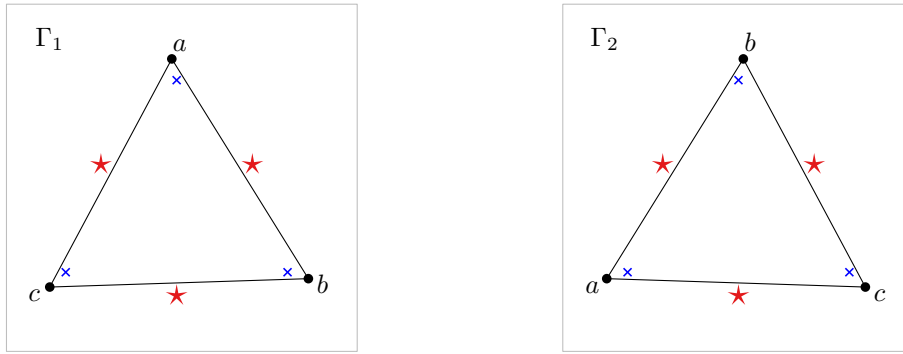


Figure 1: Two distinct drawings Γ_1 and Γ_2 of a plane cycle (a, b, c) and a set P consisting of three internal obstacles (blue crosses) and three external obstacles (red stars), which are compatible with Γ_1 and Γ_2 . There exists no planar morph between Γ_1 and Γ_2 that avoids P , i.e., the drawings are blocked by P . (For a formal justification, see Proposition 8.)

Other works are concerned with finding crossing-free morphs in \mathbb{R}^2 between two given drawings while preserving certain additional properties, such as convexity [4], upward-planarity [12], or edge lengths² [11, 3, 10], or with constructing crossing-free morphs in \mathbb{R}^2 that transform a given drawing to achieve certain properties, such as vertex visibilities [1] or convexity [15], while being in some sense monotonic, in order to preserve the so-called “mental map” [18] of the viewer.

Quite recent works [5, 6, 7] are concerned with transforming two drawings Γ_1 and Γ_2 in the plane into each other by means of crossing-free morphs in the space \mathbb{R}^3 . Such $2D$ – $3D$ – $2D$ morphs are always possible [7]—even if Γ_1 and Γ_2 have different combinatorial embeddings—and they sometimes require fewer morphing steps than morphs that are restricted to the plane \mathbb{R}^2 [5, 6]. Due to connections to the notoriously open UNKNOT problem, $3D$ – $3D$ – $3D$ morphs are not well understood and have, so far, only been considered for trees [5, 6].

Our model and motivation. In this paper, we introduce and study a natural variant of the 2-dimensional morphing problem: given two crossing-free straight-line drawings Γ_1 and Γ_2 as well as a finite set of points P in \mathbb{R}^2 , called *obstacles*, construct (or decide whether there exists) a crossing-free morph in \mathbb{R}^2 between Γ_1 and Γ_2 that *avoids* P . During such a morph, the drawing is not allowed to intersect any of the obstacles at any time point during the deformation. The obstacles remain stationary.

This problem arises naturally when constructing $2D$ – $3D$ – $2D$ morphs, where it is tempting to apply strategies for the classical 2-dimensional case on a subdrawing induced by the subset of the vertices contained in a plane π . Note that every edge between vertices on different sides of π intersects π in a point, which then acts as an obstacle for the 2-dimensional morph.

Conventions and notation. In the remainder of the paper, we consider only morphs in the plane \mathbb{R}^2 . We write “drawing” as a short-hand for “straight-line drawing in the plane \mathbb{R}^2 ” and, similarly, we write “(planar) morph” rather than “(crossing-free) morph in \mathbb{R}^2 ”. For any positive integer n , we define $[n] = \{1, 2, \dots, n\}$.

Contribution, organization, and further terminology. Let Γ_1 and Γ_2 be two drawings of the same plane graph G , and let P be a set of obstacles. We say that Γ_1 and Γ_2 are *blocked* by P if there is no planar morph between Γ_1 and Γ_2 that avoids P (see Fig. 1 for an example). Moreover, Γ_1 and Γ_2 are *blockable* if there exists a set of obstacles that blocks them.

We investigate conditions under which drawings can or cannot be blocked. In Section 2, we provide several configurations that cannot be blocked. We start by observing that drawings of graphs without cycles (that is, forests) cannot be blocked; see Proposition 3. Thus, we concentrate mostly on the case when G may contain cycles. Recall that an obvious necessary condition for the existence of a planar morph between two drawings is that they represent the same plane graph. Interpreting the obstacles in the set P as (isolated) vertices reveals that a planar morph between Γ_1 and Γ_2 that avoids P is possible only if each obstacle $p \in P$ is located in the same face in Γ_1 and Γ_2 . However, as Fig. 2 shows, this condition is not sufficient. We say that P is *compatible* with Γ_1 and Γ_2 if there is a continuous deformation

²In the fixed edge length scenario, the drawings are also known as linkages.

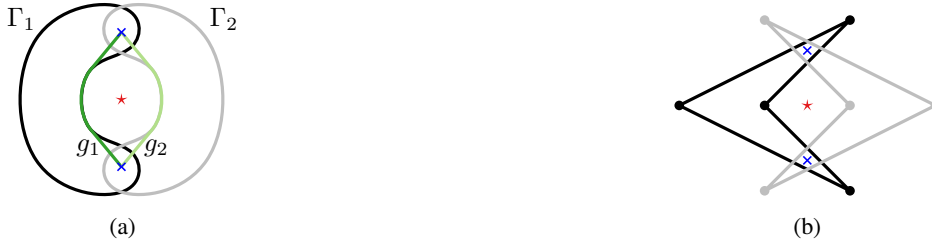


Figure 2: (a) Two simple closed curves Γ_1 and Γ_2 both containing the two obstacles marked by blue crosses and neither containing the obstacle marked by a red star. The curves Γ_1 and Γ_2 cannot be continuously deformed into each other without passing over one of the obstacles and while preserving simplicity. (The corresponding continuous deformation of the geodesic joining the two blue internal obstacles within the closed curve would transform the curve g_1 into g_2 while keeping the endpoints fixed and without passing over the red external obstacle, which is impossible.) Consequently, the two drawings of a 4-cycle in (b) are blocked by the set of three obstacles; this set is not compatible with the two drawings.

that transforms Γ_1 into Γ_2 while avoiding P and preserving pairwise noncrossing (*not necessarily straight-line*) edges at all times. The compatibility of P with Γ_1 and Γ_2 is obviously a necessary condition for the existence of a planar obstacle-avoiding morph. This condition can be checked efficiently [9, Theorem 2]; note that it is violated in Fig. 2b. We emphasize that, since the deformation in the definition of compatibility is not required to maintain straight-line edges, our necessary condition is of topological rather than geometric nature. (We remark that in the field of topology, a plane minus a finite set of obstacle points is often called a “punctured” plane. In particular, this term is used in the provided reference [9].) We show that two obstacles are never enough to block two drawings with which the obstacles are compatible, regardless of the represented graph; see Proposition 4.

Compatibility is unfortunately not sufficient for the existence of obstacle-avoiding morphs—even if the considered graph is just a (3-)cycle. We study this case in more detail. Let C_n denote the simple cycle with n vertices. Let Γ and Γ' be drawings of a plane C_n such that (i) Γ and Γ' are distinct (as mappings of C_n to the plane), but (ii) the closed curves realizing Γ and Γ' are identical, and (iii) the set of points of \mathbb{R}^2 used to represent vertices is the same in Γ and Γ' . Note that there exists an offset $o \in [n - 1]$ such that, for every $i \in [n]$, vertex i in Γ is at the same location as vertex $i + o$ (modulo n) in Γ' . Therefore, we say that Γ' is a *shifted version* of Γ , and we say that Γ and Γ' are *shifted drawings* of C_n . Due to (ii), every set of obstacles is compatible with Γ and Γ' . We conclude Section 2 by showing that multiple internal *and* external obstacles are required to block drawings of a plane C_3 (Propositions 5 and 6) and tighten these lower bounds on the number of obstacles needed to block drawings of C_3 in Section 3 by providing an example of two drawings, which are in fact shifted versions of one another (Proposition 8). In Section 4, we turn our attentions to cycles of arbitrary length. We show that a set of seven obstacles can block a morph between a drawing Γ of C_n and any shifted version Γ' of Γ ; see Proposition 9. On the other hand, we state a sufficient condition for the existence of planar obstacle-avoiding morphs between shifted drawings of C_n . We call a degree-2 vertex in a drawing *free* if its two incident edges lie on a common line. We show that if there is a free vertex in a drawing Γ of C_n , a morph between Γ and its shifted version cannot be blocked (regardless of the number of obstacles); see Proposition 10. Free vertices are helpful in other specific cases as well (in particular, they play a crucial role in the upcoming Theorem 1), but their usefulness is limited in general: their existence is not a sufficient condition for the existence of obstacle-avoiding morphs even when it comes to (nonshifted drawings of) plane cycles; see Fig. 3.

As our main result, we show that even if the compatibility condition is satisfied, it is NP-hard to decide whether an obstacle-avoiding planar morph exists (see Section 5). In fact, this statement remains true even in the severely restricted special case where only three vertices have to change positions:

Theorem 1. *Given a plane graph G , a set of obstacles P , and two crossing-free straight-line drawings Γ and Γ' of G in \mathbb{R}^2 , it is NP-hard to decide whether there exists an obstacle-avoiding crossing-free morph in \mathbb{R}^2 between Γ and Γ' . The problem remains NP-hard when restricted to the case where G is connected, the drawings Γ and Γ' are identical except for the positions of three vertices, and the obstacles P are compatible with Γ and Γ' . (These statements hold regardless of whether the morph is required to be piecewise linear or not.)*

To prove Theorem 1, we had to overcome the somewhat intricate challenge of designing gadgets that behave in a synchronous way. We conclude the paper by discussing several open questions in Section 6.

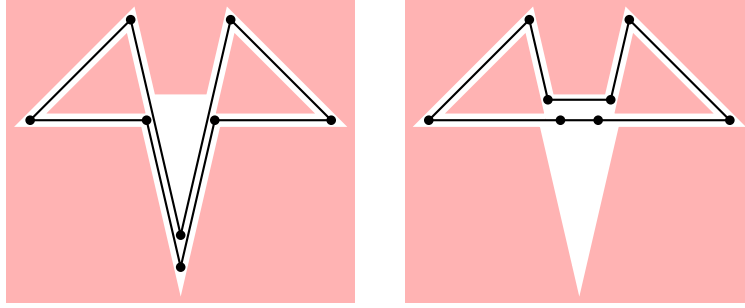


Figure 3: Two drawings of C_8 . If the (red) shaded regions are densely filled with obstacles, the drawing on the left is essentially locked in place—it cannot be morphed planarly to a substantially different drawing without intersecting the obstacle regions. In particular, it cannot be morphed to the drawing on the right, even though the right drawing contains two free vertices (and the obstacles are compatible with the two drawings).

We remark that there is no meaningful difference between piecewise linear morphs and “general” morphs – as long as one is not interested in bounding the number of morphing steps (which we are not). Thus, all of our positive results also hold when insisting on piecewise linear morphs.

Observation 2. *If there exists a planar morph between two given drawings Γ_1 and Γ_2 , then there also exists a piecewise linear planar morph between Γ_1 and Γ_2 (with possibly many steps). The same statement is true for obstacle-avoiding planar morphs since the region in which the drawing is allowed to move is open (i.e., the drawing is not allowed to intersect the obstacle points).*

2. Non-Blockable Configurations

In this section, we describe several configurations (combinations of graph classes and numbers of obstacles) that always allow planar obstacle-avoiding morphs. First, we show that trees are not blockable regardless of the number of obstacles.

Proposition 3. *Let Γ_1 and Γ_2 be two drawings of the same plane forest F . Then Γ_1 and Γ_2 are not blockable.*

Proof. We describe how to construct a morph that avoids an arbitrary finite set of obstacles. Assume for now that F consists of a single tree T , which we root at an arbitrary vertex r . We construct an obstacle-avoiding planar morph from Γ_1 to a drawing Γ'_1 located in a disk that is centered on the position of r in Γ_1 , contains no obstacles, and whose radius is smaller than the distance γ between any pair of obstacles. This can be done by “contracting” the tree along its edges in a bottom-up fashion (i.e., starting from the leaves); we discuss this process in more detail below. We also morph Γ_2 into an analogously defined drawing Γ'_2 . The drawings can now be translated (far enough) away from the obstacles without intersecting them so that they can be transformed into each other by means of morphing techniques for the classical non-obstacle case [2, 16]. The combination of these three morphs yields the desired morph from Γ_1 to Γ_2 .

If F contains multiple trees, it is easy to augment Γ_1 and Γ_2 to drawings of the same plane tree by inserting additional vertices and edges, thus, reducing to the case of a single tree.

Contraction. It remains to discuss the aforementioned contraction step. To this end, it suffices to prove the following statement.

Let v be a vertex of T (which is rooted at r), and let $T(v)$ be the subtree of T rooted at v . Further, let Γ be a drawing of T , and let ε be a positive number such that the disk $B(v, \varepsilon)$ of radius ε centered on v contains no obstacle and no vertex other than v and intersects only edges that are incident to v . Then there is a planar obstacle-avoiding morph from Γ to a drawing Γ^ν of T in which the subdrawing of $T(v)$ is located in $B(v, \varepsilon)$. Further, v and all vertices that do not belong to $T(v)$ are placed exactly as in Γ .

Note that, indeed, by choosing $\varepsilon < \gamma$ and $\Gamma = \Gamma_1$, the drawing Γ^ν corresponds to the desired drawing Γ'_1 .

We prove the statement by induction on the height of $T(v)$. If v is a leaf, the statement follows trivially. So suppose v is not a leaf. Let c_1, c_2, \dots, c_k be the children of v . For every $i \in [k]$, we choose a radius $\delta_i \ll \varepsilon$ such that the

disk $B(c_i, \delta_i)$ contains no vertex other than c_i , intersects only edges incident to c_i , and can be translated in direction $\overline{c_i v}$ until it is fully contained in $B(v, \varepsilon)$ without intersecting any obstacles or edges of Γ that are not incident to vertices of $T(c_i)$. Moreover, we choose these radii small enough such that when carrying out these translations simultaneously, the disks $B(c_i, \delta_i)$ do not intersect each other. Clearly, such a set of radii exists. Now we can inductively contract each subtree $T(c_i)$ into its disk $B(c_i, \delta_i)$ and simultaneously apply the described translations to obtain the desired morph to the drawing Γ^v . \square

Now we show that two obstacles are not enough to block two drawings (with which the obstacles are compatible), regardless of the represented graph. The main idea of the proof is as follows: we interpret the obstacles as (isolated) vertices of our graph and use previous results to determine an “ordinary” planar morph (in which the obstacles move). We then transform this morph into the desired obstacle-avoiding morph by translating, rotating, and scaling the frame of reference as time goes on to ensure that the obstacles become fixed points (one can think of this as moving, rotating, and zooming the camera in a suitable fashion).

Proposition 4. *Let Γ_1 and Γ_2 be two drawings of the same plane graph G , and let P be a set of obstacles that are compatible with Γ_1 and Γ_2 . If $|P| \leq 2$, then there exists a planar morph from Γ_1 to Γ_2 that avoids P .*

Proof. We show the statement for a set $P = \{p_1, p_2\}$ of size 2. The case $|P| = 1$ can be treated as the case $|P| = 2$ by placing a second obstacle in the vicinity of the first one.

Without loss of generality, we assume that $d(p_1, p_2) = 1$. Let G' be the plane graph obtained from G by introducing two new isolated vertices v_1 and v_2 and assigning them into the faces where the obstacles p_1 and p_2 lie in Γ_1 (and thus also in Γ_2). Let Γ'_1 and Γ'_2 be the drawings of G' that are obtained from Γ_1 and Γ_2 , respectively, by placing v_1 and v_2 at the positions of p_1 and p_2 , respectively.

We know that there exists a morph M_1 from Γ'_1 to Γ'_2 [2, 16]. We can treat M_1 as a continuous function from the interval $[0, 1]$ onto the set of straight-line drawings of G' such that $M_1(0) = \Gamma'_1$ and $M_1(1) = \Gamma'_2$. Since M_1 is continuous, the function $s : [0, 1] \rightarrow \mathbb{R}^2$ that describes the position of v_1 in \mathbb{R}^2 relative to its starting point during the morph M_1 is continuous as well, and since v_1 is drawn at the same position in Γ'_1 and Γ'_2 , we know that $s(0) = s(1) = (0, 0)$. We now define a new morph M_2 that is obtained from M_1 by translating $M_1(x)$ by the vector $-s(x)$ for every $x \in [0, 1]$. Then M_2 is a continuous morph from Γ'_1 to Γ'_2 , and, for every $x \in [0, 1]$, in the drawing $M_2(x)$, the vertex v_1 is placed at p_1 .

In the same manner, we define the function $t : [0, 1] \rightarrow \mathbb{R}_{>0}$ that describes the distance between v_1 and v_2 in $M_2(x)$ for every $x \in [0, 1]$. Since $d(p_1, p_2) = 1$, we know that $t(0) = t(1) = 1$, and t is continuous since M_2 is continuous. We define a new morph M_3 that is obtained from M_2 by scaling $M_2(x)$ by the factor $1/t(x)$ around the point v_1 for every $x \in [0, 1]$. Then M_3 is a continuous morph from Γ'_1 to Γ'_2 that keeps v_1 fix, and the distance between v_1 and v_2 is equal to 1 in $M_3(x)$ for every $x \in [0, 1]$.

We define a third function $\rho : [0, 1] \rightarrow \mathbb{R}_{>0}$ that describes, for every $x \in [0, 1]$, in $M_2(x)$ the angle between the horizontal ray that emanates from v_1 and points to the right and the ray from v_1 to v_2 . Since v_1 and v_2 are in the same positions in Γ'_1 and Γ'_2 , we know that $\rho(0) = \rho(1) = 0$, and ρ is continuous since M_3 is continuous. We define a new morph M_4 that is obtained from M_3 by rotating $M_3(x)$ around v_1 by an angle of $-\rho(x)$ for every $x \in [0, 1]$. Then M_4 is a continuous morph from Γ'_1 to Γ'_2 , where v_1 is fix, the distance between v_1 and v_2 equals 1 in $M_4(x)$ for every $x \in [0, 1]$, and the ray from v_1 to v_2 does not change its slope during the morph. Thus, v_2 , too, is fix under M_4 . Then, if we restrict M_4 to G , we obtain a morph from Γ_1 to Γ_2 that avoids P , which proves the statement for $|P| = 2$. \square

In the remainder of this section, we focus on the case where the graph is a 3-cycle. In particular, in the following two propositions, we show that a set of compatible obstacles that blocks drawings of C_3 has to contain multiple internal and multiple external obstacles. As we will show in Section 3, the bounds on the number of internal and external obstacles in these propositions are best-possible.

Proposition 5. *Let Γ_1 and Γ_2 be drawings of a plane C_3 , and let P be a set of obstacles compatible with Γ_1 and Γ_2 . If at most one obstacle of P lies in the exterior of Γ_1 (and Γ_2), then there is a planar morph from Γ_1 to Γ_2 that avoids P .*

Proof. Our strategy is as follows: we first define a set of canonical drawings, then show how to transform any two canonical drawings into each other and, finally, describe how each of the given drawings can be transformed into a canonical drawing. The combination of these three morphs yields the desired morph between Γ_1 and Γ_2 .

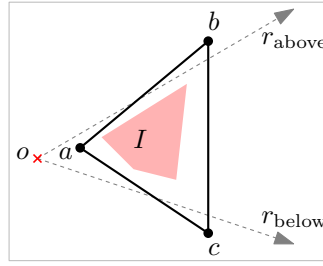


Figure 4: Construction of the canonical triangle.

We describe our approach assuming that there is an external obstacle (if this not the case, one can simply pick an arbitrary point in the exterior of both drawings and, interpreting this point as an (external) obstacle, execute the same strategy).

Canonical drawings. The following construction is illustrated in Fig. 4. Let $o = (x_o, y_o)$ denote the external obstacle and its coordinates and let I denote the set of internal obstacles. Without loss of generality, we may assume that x_o is strictly smaller than the x-coordinate of all internal obstacles. (Note that o lies in the exterior of the convex hull of I and, hence, there exists a line that separates o from I . By applying a suitable rotation of the plane, we may assume this line to be vertical and o to be to its left.) Let r_{above} be a ray that originates at o and lies above all internal obstacles. Symmetrically, let r_{below} be a ray that originates at o and lies below all internal obstacles. Note that the direction vector of both rays has a positive x-coordinate. Let $a = (x_a, y_a)$, $b = (x_b, y_b)$, and $c = (x_c, y_c)$ be points (and their coordinates) such that

- x_a is strictly smaller than the x-coordinate of all internal obstacles, but strictly larger than x_o ;
- x_b is strictly larger than the x-coordinate of all internal obstacles;
- $x_c = x_b$;
- a lies below r_{above} and above r_{below} ;
- b lies above r_{above} and such that the line through a and b is above all obstacles; and
- c lies below r_{below} and such that the line through a and c is below all obstacles.

We use ℓ_{ab} to denote the line through a and b ; the lines ℓ_{bc} and ℓ_{ac} are defined analogously. Note that all internal obstacles are located in the interior of the triangle abc while o is located in the exterior of abc . More precisely, the external obstacle o is located above ℓ_{ab} and below ℓ_{ac} .

Any drawing of our plane 3-cycle in which the vertices are placed at a , b , and c is called *canonical*. Thus, there are three distinct canonical drawings (taking into account shifted versions).

Morphing between canonical drawings. Let Γ be a canonical drawing with vertices v, w, u at a, b, c , respectively. We show how to morph to a shifted (canonical) drawing of Γ . (By repeating the described strategy once more, one can obtain a morph to the third canonical drawing.) The process is visualized in Fig. 5.

Let p_v, p_u be points such that

- p_v lies on ℓ_{ac} and its x-coordinate is strictly smaller than x_a ;
- p_u lies on ℓ_{ab} and its x-coordinate is strictly smaller than x_a ; and
- the lines $\ell_{p_v b}$ and $\ell_{p_u c}$ through p_v, b and p_u, c , respectively, intersect in a point whose x-coordinate is strictly larger than $x_b (= x_c)$.

We use p_w to denote the intersection point of $\ell_{p_v b}$ and $\ell_{p_u c}$.

We proceed in five simple steps. It is readily observed from properties of the triangle abc and the definitions of p_v, p_u, p_w that all of these steps are obstacle-avoiding and planar.

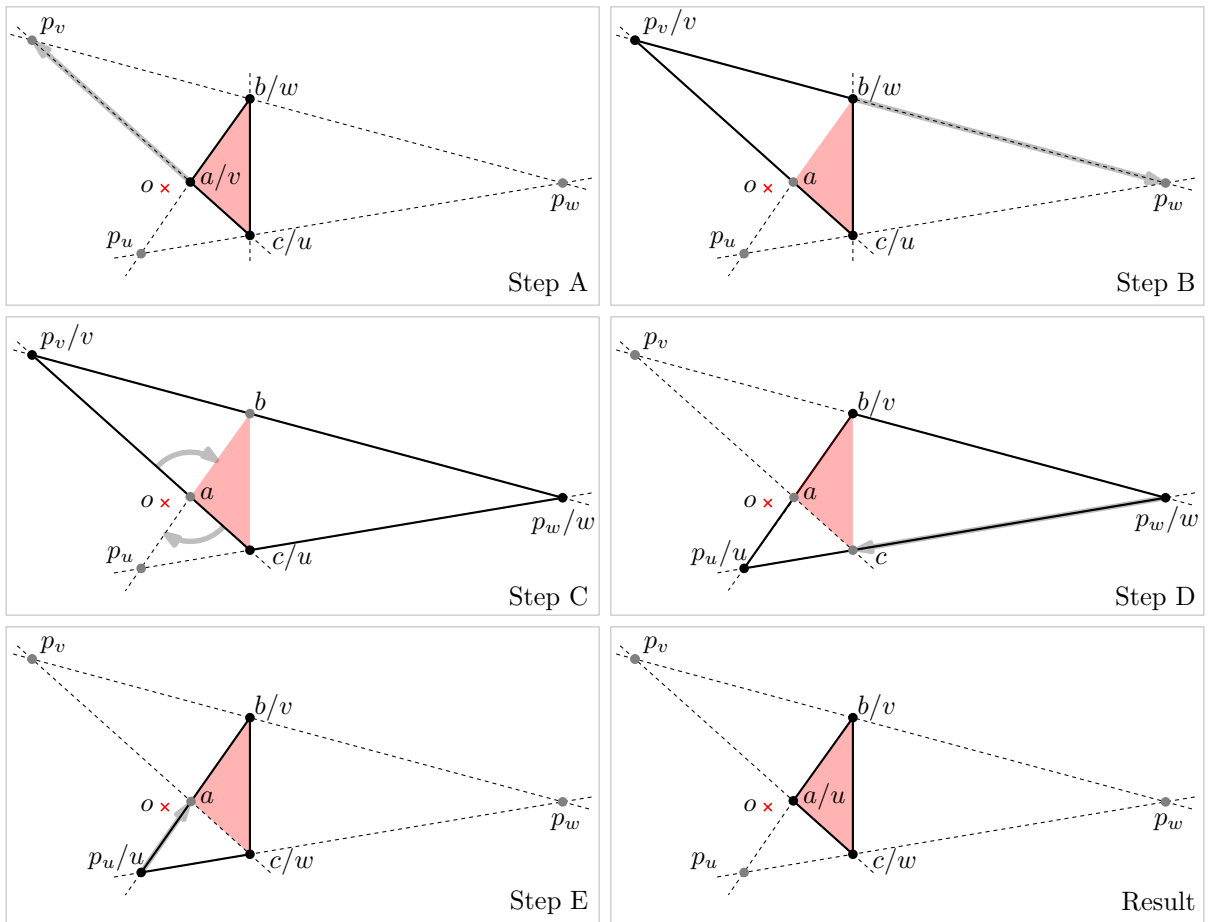


Figure 5: A morph of a canonical drawing of a 3-cycle with vertices u, v, w placed at c, a, b , respectively, to a shifted version where the vertices are placed at a, b, c , respectively. In the subfigures, we used the notation x/y to mean that vertex y is placed at point x .

- Step A. We use a linear morph to move v to p_v .
- Step B. We use a linear morph to move w to p_w .
- Step C. We simultaneously move u to p_u along up_u and v to b along $p_v b$ and do so in a way where the intersection point of the edge uv with ℓ_{ab} remains at a . (Essentially, we rotate uv around fixpoint a and simultaneously change its length to ensure that u and v move along the desired segments. We remark that this is not necessarily a linear morph.)
- Step D. We use a linear morph to move w to c .
- Step E. We use a linear morph to move u to a .

Morphing to canonical drawings. Let $\Gamma \in \{\Gamma_1, \Gamma_2\}$. Let \triangle be a triangle that has all internal vertices in its interior and o in its exterior. We describe an obstacle-avoiding planar morph that transforms Γ such that its vertices lie at the corners of \triangle (in particular, this means we can morph to a canonical drawing). The process is visualized in Fig. 6.

Let e be an edge of Γ such that its supporting line ℓ has the property that o is on the side of ℓ that does not contain the internal obstacles. Define an edge (side) \hat{e} of \triangle and its supporting line $\hat{\ell}$ analogously. We may assume that ℓ and $\hat{\ell}$ are not parallel, otherwise we can simply use a morph to slightly move one of the endpoints of e to ensure this is the case (this can obviously be done in an obstacle-avoiding planar fashion). Further, we may assume without loss of generality (by rotating and / or reflecting the plane if necessary) that ℓ is vertical, o is to the left of ℓ , and o is above $\hat{\ell}$. By construction, the lines ℓ and $\hat{\ell}$ partition the plane into four regions, which we denote as follows:

- R_o^{tl} is to the left of ℓ , above $\hat{\ell}$, and contains o ;
- R_\emptyset^{tr} is to the right of ℓ , above $\hat{\ell}$, and contains no obstacles;
- R_I^{br} is to the right of ℓ , below $\hat{\ell}$, and contains all internal obstacles; and
- R_\emptyset^{bl} is to the left of ℓ , below $\hat{\ell}$, and contains no obstacles.

Let x denote the point where ℓ and $\hat{\ell}$ cross. Let D be a disk centered on x that contains Γ and \triangle in its interior. Let u and v be the top and bottom endpoint of e , respectively. Let w denote the remaining vertex of Γ (which lies to the right of ℓ). We proceed in several steps:

- Step 1 Let ℓ'_{uw} be a line that is parallel to the edge uw and that lies above D . Symmetrically, let ℓ'_{vw} be a line that is parallel to the edge vw and that lies below D . Let u' denote the point where ℓ and ℓ'_{uw} cross. Let v' denote the point where ℓ and ℓ'_{vw} cross. Finally, let w' denote the point where ℓ'_{uw} and ℓ'_{vw} cross. We use a single linear morph to move u to u' , v to v' , and w to w' . Note that this morph “expands” our drawing, that is, the initial drawing is contained in the interiors of the final drawing and all intermediate drawings. Hence, it avoids the internal obstacles. Moreover, the drawing remains in the half-plane to the right of ℓ and, thus, the external obstacle o is also avoided.
- Step 2 Note that the edges uw and vw are now in the exterior of D . We use a morph to rotate our drawing clockwise around fixpoint x until the edge uw lies on $\hat{\ell}$. During this rotation, the edges uw and vw remain in the exterior of D and, thus, avoid all internal obstacles (which all lie in the interior of D). Moreover, the edges uw and vw never enter the region R_o^{tl} and, thus avoid the external obstacle o . The supporting line of the edge uw covers exactly the regions R_\emptyset^{tr} and R_\emptyset^{bl} during the rotation. Thus, the edge uw also avoids all obstacles.
- Step 3 We use a linear morph to move w to the corner of \triangle that does not lie on $\hat{\ell}$. It is easy to see that this morph is obstacle-avoiding and planar.
- Step 4 We use a linear morph to move u to the right corner of \triangle on $\hat{\ell}$ and v to the left corner of \triangle on $\hat{\ell}$. It is easy to see that this morph is obstacle-avoiding and planar.

Morphing Graph Drawings in the Presence of Point Obstacles

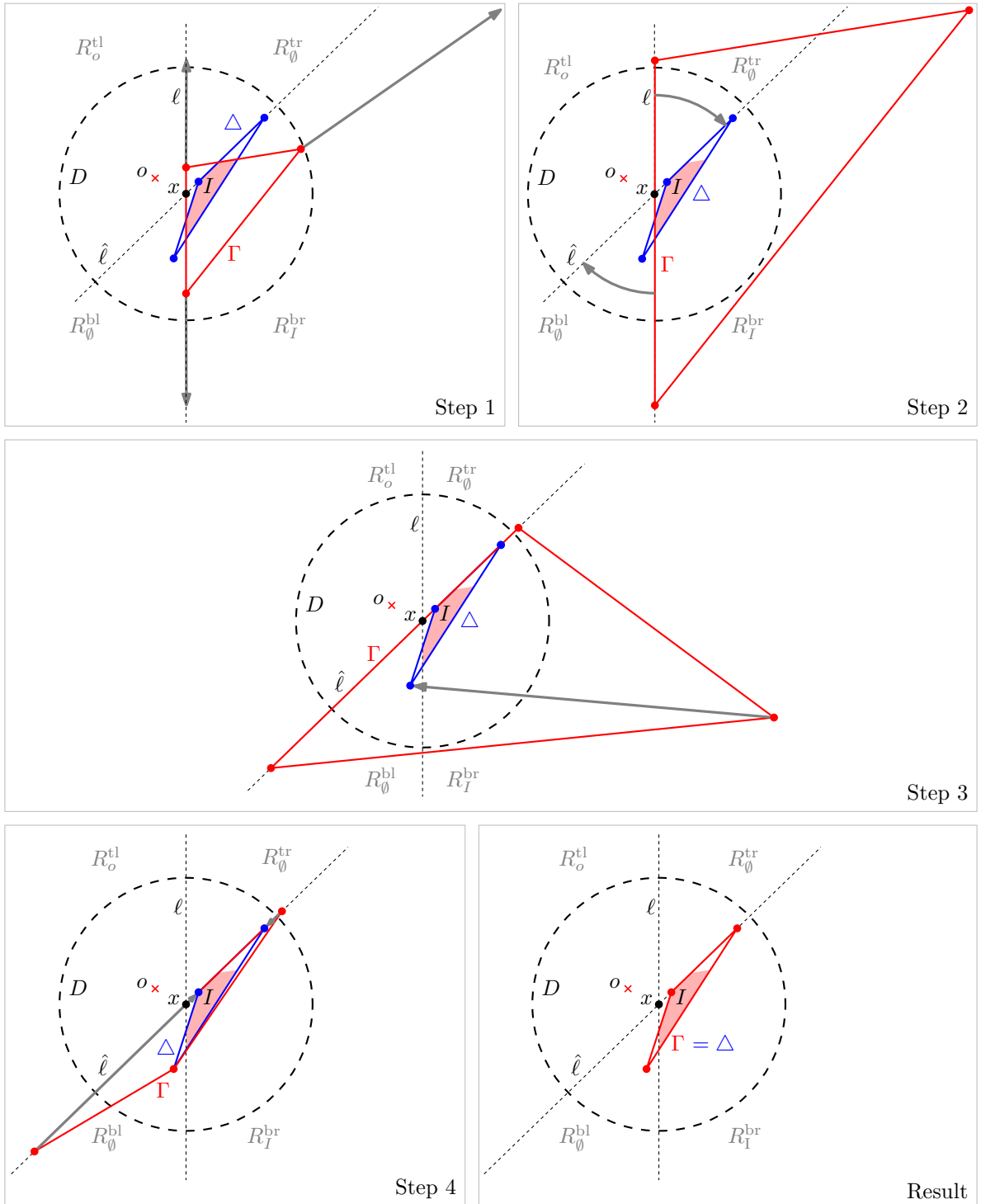


Figure 6: A morph transforming Γ so that its vertices lie on the corners of a triangle Δ .

Wrap-up. We have described how to transform both Γ_1 and Γ_2 into canonical drawings and how canonical drawings can be transformed into each other. In combination, this yields the desired morph. \square

Proposition 6. *Let Γ_1 and Γ_2 be drawings of a plane C_3 , and let P be a set of obstacles compatible with Γ_1 and Γ_2 . If at most two obstacles of P lie in the interior of Γ_1 (and Γ_2), then there is a planar morph from Γ_1 to Γ_2 that avoids P .*

Proof. Our strategy is similar to the one used in Proposition 5: we construct a rectangle that contains both internal obstacles and that is in the interior of both drawings. We then describe how each of our drawings can be transformed such that its vertices lie on the boundary of the rectangle. Finally, we describe how to morph between the resulting two drawings. The combination of these three morphs yields the desired morph between Γ_1 and Γ_2 .

We describe our approach assuming that there are exactly two internal obstacles. If there is only one internal obstacle, we can pick an arbitrary point interior to both drawings and, interpreting this point as an additional (internal) obstacle, execute the same strategy. Similarly, if there is no internal obstacle, we can simply shrink the drawing Γ_1 (by moving all of its vertices close to some point in its interior), use a sequence of translations to move it into the interior of Γ_2 without intersecting any obstacles, pick two arbitrary points in the interior of both drawings, and, interpreting these points as (internal) obstacles, execute our strategy for two internal obstacles.

We begin by introducing some notation.

Setup. For illustrations of the notation introduced in this paragraph, refer to Fig. 7. We let $p_a = (x_a, y_a)$ and $p_b = (x_b, y_b)$ denote the internal obstacles and their coordinates. Without loss of generality, we assume that $x_a = x_b$ and $y_a > y_b$. Choose an $\varepsilon > 0$ such that the rectangle $R = [x_a - \varepsilon, x_a + \varepsilon] \times [y_b - \varepsilon, y_a + \varepsilon]$ is contained in the interior of both Γ_1 and Γ_2 . Let ℓ , m , and r denote the vertical lines with x-coordinates $x_\ell = x_a - \varepsilon$, $x_m = x_a$, and $x_r = x_a + \varepsilon$, respectively. Let $\Gamma \in \{\Gamma_1, \Gamma_2\}$, and let $u = (x_u, y_u)$, $v = (x_v, y_v)$, and $w = (x_w, y_w)$ denote (the coordinates of) its vertices. Note that Γ intersects m in exactly two points. In other words, one of its three edges, say uv , lies completely in one of the two closed half-planes bounded by m and the other two edges each intersect m in a single point (possibly an endpoint). By suitably reflecting the plane and relabeling obstacles and / or vertices if necessary, we may assume that

- if one endpoint of uv lies on m , then this endpoint is v ;
- uv lies in the closed half-plane to the left of m , i.e., $x_u < x_m$, $x_v \leq x_m$ (and, consequently $x_r < x_w$); and
- the edge vw intersects m above R and the edge uw intersects m below R .

Moving the vertices onto the boundary of the rectangle. We now describe an obstacle-avoiding planar morph that transforms Γ into a drawing whose vertices lie on the boundary of R . It consists of several basic steps, which are illustrated in Fig. 7:

- Step 1. Move v along vw to the intersection of vw with m (which is above R). Note that the (triangular) convex hull of the old and new drawing of uv (this is the region covered by uv during this morph) does not contain any obstacle or w , so this morph is planar and obstacle-avoiding.
- Step 2. Move v downwards along m to the top boundary of R . Note that the (triangular) convex hull of the old and new drawing of uv does not contain any obstacle or w and the (triangular) convex hull of the old and new drawing of vw does not contain any obstacle or u , so this morph is planar and obstacle-avoiding.
- Step 3. Move w along uw to the intersection of uw with r (which is below R). Note that the (triangular) convex hull of the old and new drawing of vw does not contain any obstacle or u , so this morph is planar and obstacle-avoiding.
- Step 4. Move u along uw until it lies in the closed vertical slab bounded by ℓ and m ; it then lies below R (we remark that it is possible for u to lie in this slab to begin with). Note that the (triangular) convex hull of the old and new drawing of uv does not contain any obstacle or w , so this morph is planar and obstacle-avoiding.
- Step 5. Finally, move u along uw and w along vw until they reach the bottom segment of R . Note that the (quadrangular) convex hull of the old and new drawing of uw does not contain any obstacle or v , so this morph is planar and obstacle-avoiding.

Let Γ' denote the result drawing.

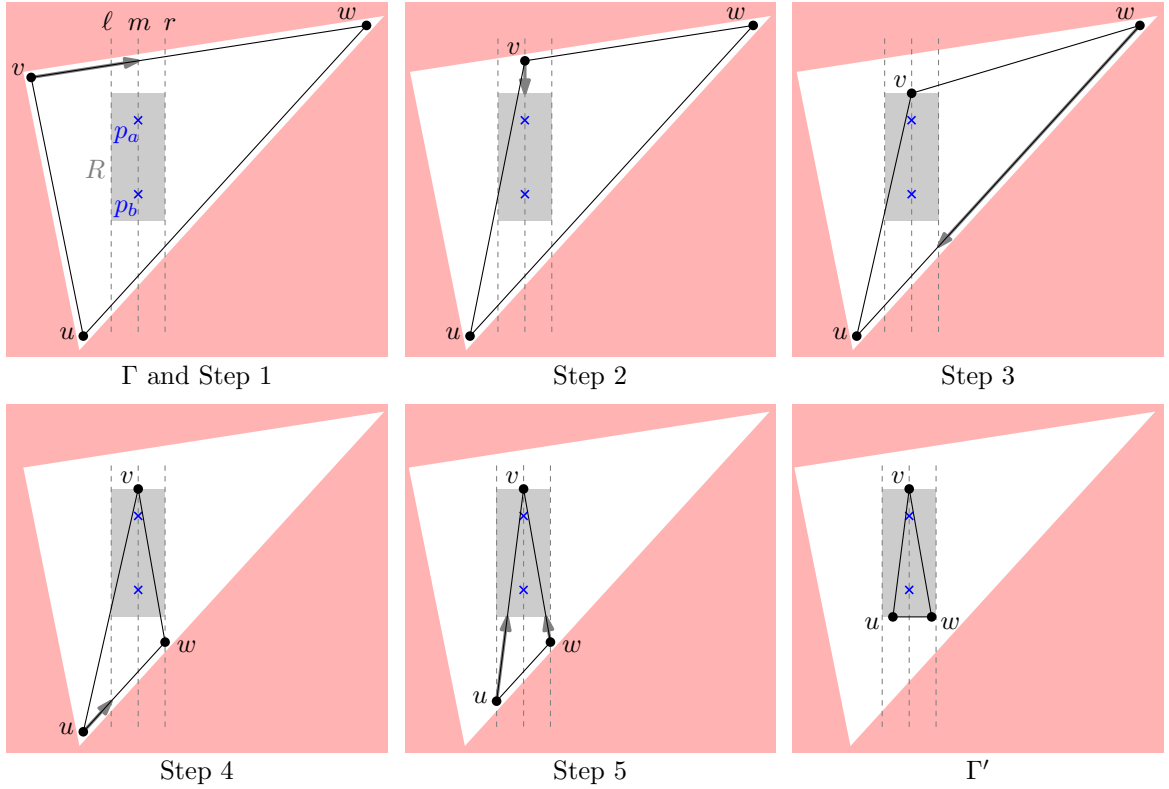


Figure 7: Our strategy for morphing the vertices of Γ onto the boundary of the rectangle R in the proof of Proposition 6. The resulting morph avoids the exterior of the initial drawing (shaded) entirely and can hence be applied regardless of the number and placement of the external obstacles.

Morphing to and between canonical drawings. We say that a drawing of our plane 3-cycle is *canonical* if its vertices are placed either at $R_{bl} = (x_b - \varepsilon, y_b - \varepsilon)$, $R_{br} = (x_b + \varepsilon, y_b - \varepsilon)$, and $R_{tm} = (x_a, y_a + \varepsilon)$, or, symmetrically, at $R_{tl} = (x_a - \varepsilon, y_a + \varepsilon)$, $R_{tr} = (x_a + \varepsilon, y_a + \varepsilon)$, and $R_{bm} = (x_b, y_b - \varepsilon)$. Taking into account shifted drawings, there are thus 6 canonical drawings in total.

It is easy to transform our drawing Γ' into a canonical one: vertex v is already located at R_{tm} and the other two vertices are located on the bottom segment of R (with u to the left of w). Thus, we can simply move u to R_{bl} and w to R_{br} along the bottom segment of R . Moreover, we can now easily transform the resulting canonical drawing Γ'' into any other canonical drawing: first, we slightly increase the x-coordinate of v while maintaining the property that the line through u and v is above the obstacles p_a and p_b . Second, we move w to R_{bm} . Third, we move u to R_{tl} . Finally, we move v to R_{tr} . In each step, the (triangular) convex hull of the old and new version of redrawn edge does not contain any obstacles or the nonincident vertex, so all these morphing steps are planar and obstacle-avoiding. By repeating (a symmetric version of) this strategy, we can reach any canonical drawing, as claimed.

Wrap-up. We have described how to transform both Γ_1 and Γ_2 into canonical drawings and how canonical drawings can be transformed into each other. In combination, this yields the desired morph. \square

3. A Tight Lower Bound on the Number of Obstacles to Block Drawings of 3-Cycles

In this section, we establish a tight lower bound on the number of obstacles needed to block (shifted) drawings of C_3 .

Proposition 7. *Let Γ_1 and Γ_2 be drawings of a plane C_3 , and let P be a set of obstacles compatible with Γ_1 and Γ_2 . If Γ_1 and Γ_2 are blocked by P , then P contains at least five obstacles (three of which are internal and two of which are external).*

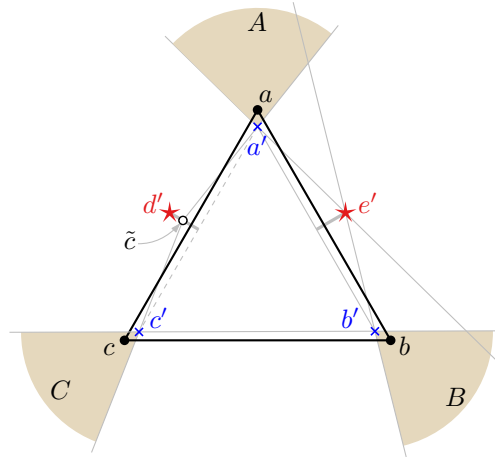


Figure 8: Five obstacles suffice to block shifted versions of C_3 .

Proof. Follows immediately from Propositions 5 and 6. \square

Proposition 8. *Let Γ be a drawing of C_3 , and let Γ' be a shifted version of Γ . Then Γ and Γ' are blockable by five obstacles (three of which are internal and two of which are external) compatible with Γ and Γ' .*

If Γ is an isosceles triangle where the base has length s , then it suffices to place the internal obstacles at a distance of at most $s/12$ next to the three vertices and the external obstacles at a distance of at most $s/12$ next to the midpoints of the two legs.

Proof. Let a , b , and c be the vertices of C_3 . We put three obstacles a' , b' , and c' in the inner face of Γ in the vicinity of the corresponding vertices, i.e., inside a disk of radius $\varepsilon > 0$, where ε is much smaller than the length of any edge of Γ ; see Fig. 8. We put the other two obstacles d' and e' in the outer face of Γ , namely in the ε -vicinity of the midpoints of the edges ac and ab , respectively. We show by contradiction that this set of obstacles blocks any morph between Γ and Γ' .

Without loss of generality, we may assume that a is the vertex of C_3 with the largest y -coordinate in Γ , that b lies on the right side of the vertical line through a , and that c lies on the left side. We may also assume that ε is chosen so small that the line $c'd'$ has positive slope and the line $b'e'$ has negative slope. This implies that b' lies on the right side and that c' lies on the left side of the vertical line through a .

Now suppose, for a contradiction, that there is a morph from Γ to a shifted version Γ' such that c is the vertex with largest y -coordinate in Γ' . Note that during this morph no edge of the triangle $\triangle abc$ may intersect the triangle $\triangle a'b'c'$ because $\triangle abc$ must always contain a' , b' , and c' . Hence, on the way from its initial to its final position, vertex c must go around $\triangle a'b'c'$ either clockwise (near d') or counterclockwise (near e'). We assume that c goes clockwise; the other case is symmetric.

Consider the intermediate drawing $\tilde{\Gamma}$ where c lies on the normal of the edge ac through d' in Γ . Let \tilde{a} , \tilde{b} , and \tilde{c} be the positions of a , b , and c in $\tilde{\Gamma}$, respectively. On the normal of ac , \tilde{c} must lie between d' and the intersection point with $a'c'$. For the edge $\tilde{c}\tilde{a}$ not to intersect $\triangle a'b'c'$, \tilde{a} must lie above the line $\tilde{c}a'$; see Fig. 8. To ensure that b' lies inside $\triangle \tilde{a}\tilde{b}\tilde{c}$, the point \tilde{b} must be below the line $b'e'$. Similarly, the point \tilde{a} must lie above the line $a'e'$ to ensure that e' lies outside $\triangle \tilde{a}\tilde{b}\tilde{c}$. Hence \tilde{a} must lie inside the wedge A with apex a' that is the intersection of the two halfplanes above the lines $\tilde{c}a'$ and $e'a'$. Similarly, from the point of view of \tilde{c} , the point \tilde{b} must lie in the wedge C with apex c' that is the intersection of the two halfplanes below the line $b'e'$ and the halfplane to the left of the line $c'\tilde{c}$. To ensure that e' lies outside $\triangle \tilde{a}\tilde{b}\tilde{c}$, however, the point \tilde{b} must lie to the right of the line $b'e'$. This forces \tilde{b} to lie in the wedge B with apex b' , that is, the intersection of the halfplane below $b'e'$ and the halfplane to the right of $e'b'$. Hence \tilde{b} must lie in $B \cap C$. However, the apices b' and c' of B and C , respectively, lie on different sides of the vertical line through a . Moreover, the left boundary of B is part of the line $b'e'$, whose slope we assumed to be negative, and the slope of the right boundary of C is less than the slope of the line $c'd'$, which we assumed to be positive. Therefore, B lies completely to the right of the vertical line through a , whereas C lies completely to the left of this line.

Hence, the intermediate drawing $\tilde{\Gamma}$ cannot exist, and Γ and Γ' are blocked by the set of obstacles.

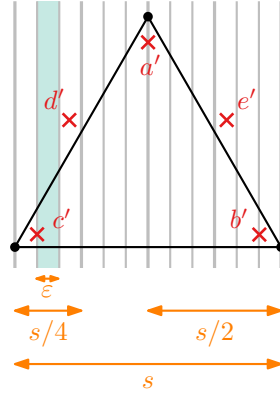


Figure 9: If we place the obstacles as described in the proof of Proposition 8 in ε distance around an isosceles triangle with side lengths s , then it suffices to set $\varepsilon = s/12$ to ensure that the line segment $c'd'$ has positive slope.

Finally, we argue about the precise placement of the obstacles stated above if Γ is an isosceles triangle whose base has length s . To this end, we show how to choose ε sufficiently small. Without loss of generality, we assume that bc is the base and bc is drawn horizontally in Γ . The only requirement to ε is that the lines $c'd'$ and $b'e'$ have a positive and a negative slope, respectively. If we set $\varepsilon = s/12$, it is easy to see that these requirements are fulfilled: if we divide the drawing into vertical strips of width $s/12$, then c' is in a strip to the left of d' , and e' is in a strip to the left of b' ; see Fig. 9. \square

4. Shifted Versions of Cycles with and without Free Vertices

In this section, we investigate (shifted) drawings cycles of arbitrary length. We start by showing that it is not always possible to morph between a drawing of C_n and a shifted version of this drawing in an obstacle-avoiding fashion.

Proposition 9. *Let $n \geq 6$ be an even integer. Then there exists a drawing Γ of C_n such that, for every shifted version Γ' of Γ , the drawings Γ and Γ' are blockable by seven obstacles that are compatible with Γ and Γ' .*

Proof. Let Γ be a drawing of C_n that it is wrapped around an imaginary equilateral triangle \triangle formed by the positions of the first three vertices of C_n ; see Fig. 10. We place \triangle such that its bottom edge is horizontal. We start with the first vertex v_1 of C_n in the lower right corner of \triangle . Then, in $n/2$ steps, we go clockwise around (the corners of) \triangle . In the i -th step, we place v_{i+1} and v_{n-i+1} near the currently considered corner of \triangle such that the two new vertices see their predecessors (and will see their successors) and lie slightly further away from the barycenter of \triangle than the other vertices that we have placed near the same corner of \triangle . We can place the vertices of C_n (and four of the obstacles, see below) such that each of them lies within a radius- ε disk centered at one of the corners of \triangle , for some $\varepsilon > 0$. These radius- ε disks correspond to the shaded green areas in the schematic drawing in Fig. 10.

We place two obstacles in the interior of C_n , namely in the immediate vicinity of v_1 and $v_{n/2+1}$ (see the blue crosses in Fig. 10). Additionally, we place five obstacles in the complement of C_n (see the red stars in Fig. 10). First, we place two of these in the immediate vicinity of v_2 and v_3 (closer to v_2 and v_3 than to v_n and v_{n-1} , respectively). Then, we place the remaining three obstacles very close to the midpoints of the three outermost edges of C_n (that is, $v_{n/2+1}v_{n/2+2}$, $v_{n/2+2}v_{n/2+3}$, and $v_{n/2+3}v_{n/2+4}$). Due to the tight wrapping of C_n around \triangle and the extra obstacles on each of the three sides of the drawing, the drawing of C_n is constrained within a triangular strip of width ε around \triangle . Therefore no edge can change its slope (measured as the angle it forms with, say, the positive x-axis) by more than $O(\varepsilon)$ degrees. Hence no edge can be turned such that it aligns with one of its incident edges, which would mean to change its slope by roughly 120° . Hence, Γ and Γ' are blocked for every shifted version Γ' of Γ . \square

Observe that it is plausible that Proposition 9 can be strengthened: even three obstacles (the two internal and one external in the bottom left corner of the middle part of the drawing; see Fig. 10) seem to be sufficient for blocking two shifted drawings of an even-length cycle (we chose to use seven obstacles to simplify the proof). In view of this remark, it seems that Proposition 4 is best-possible. In particular, the proof strategy does not generalize to three obstacles as affine transformations preserve the cyclic orientations of point triples.

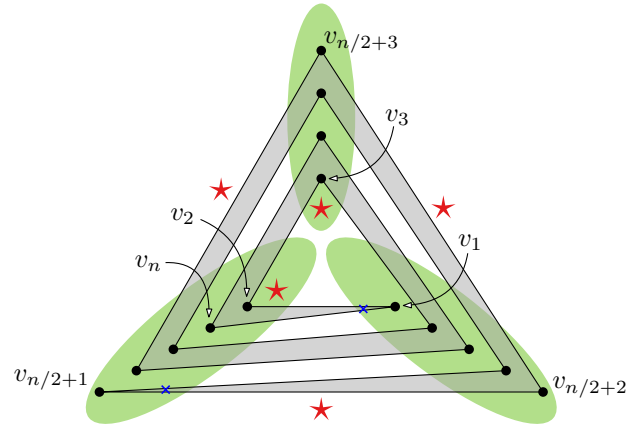


Figure 10: A schematic drawing of C_n with vertices v_1, \dots, v_n (here $n = 14$) that cannot be morphed to a shifted version of itself in a planar way while avoiding the two internal obstacles (blue crosses) and the five external obstacles (red stars). In the actual drawing, each set of vertices and obstacles contained in the same shaded green area is placed within a radius- ε disk (for some $\varepsilon > 0$) centered at a corner of an equilateral triangle with unit edge length.

Now we show that the presence of a free vertex is sufficient for the existence of planar obstacle-avoiding morphs between shifted drawings of a cycle.

Proposition 10. *Let Γ be a drawing of C_n , and let Γ' be a shifted version of Γ . If Γ contains a free vertex, then Γ and Γ' are not blockable by obstacles that are compatible with Γ and Γ' .*

Proof. Let v_0, v_1, \dots, v_{n-1} be the vertices of C_n in clockwise order around Γ such that v_0 is the free vertex. We move v_0 immediately next to v_1 such that v_1 lies on the line segment v_0v_2 . As a result, v_1 is free and can be moved very close to v_2 . We iterate this move for every vertex until v_0 becomes free again. Finally, we move, for $i \in [n-1]$, v_i very slightly to the former position of v_{i+1} and v_0 to, say, the midpoint of the line segment $v_{n-1}v_1$. Together, all these moves represent a morph from Γ to a shifted version Γ_1 of Γ , where, for every $i \in [n-2]$, vertex v_i has moved to the position of its successor v_{i+1} and vertex v_{n-1} has moved to the position of v_1 . Repeating the whole procedure as often as necessary yields a morph from Γ to any shifted version of Γ . \square

5. NP-Hardness (Proof of Theorem 1)

In this section, we show our main result.

Theorem 1. *Given a plane graph G , a set of obstacles P , and two crossing-free straight-line drawings Γ and Γ' of G in \mathbb{R}^2 , it is NP-hard to decide whether there exists an obstacle-avoiding crossing-free morph in \mathbb{R}^2 between Γ and Γ' . The problem remains NP-hard when restricted to the case where G is connected, the drawings Γ and Γ' are identical except for the positions of three vertices, and the obstacles P are compatible with Γ and Γ' . (These statements hold regardless of whether the morph is required to be piecewise linear or not.)*

Proof. We reduce from the classical NP-hard problem 3-SAT. Given a Boolean formula $\Phi = \bigwedge_{i=1}^m c_i$ in conjunctive normal form over variables x_1, x_2, \dots, x_n whose clauses c_1, c_2, \dots, c_m consist of three literals each, we construct a plane graph G , two planar drawings Γ and Γ' of G , and a set P of obstacles that are compatible with Γ and Γ' such that there exists an obstacle-avoiding planar morph from Γ to Γ' if and only if Φ is satisfiable. We proceed with a high-level overview of our construction and then discuss the individual aspects in more detail.

Overview. We arrange the obstacles of P and the vertices and edges in Γ and Γ' such that we obtain a grid-like structure where we have two rows for each variable (one for each literal of the variable) and three columns for every clause (one for each literal in the clause); see Fig. 11. We then use several gadgets arranged within this grid-like structure. On the left side, the two rows of a variable terminate at a *variable gadget*. A variable gadget is in one of the states true, false, or unset. On the top side, the three columns of a clause are joined via three *literal gadgets* to a *clause*

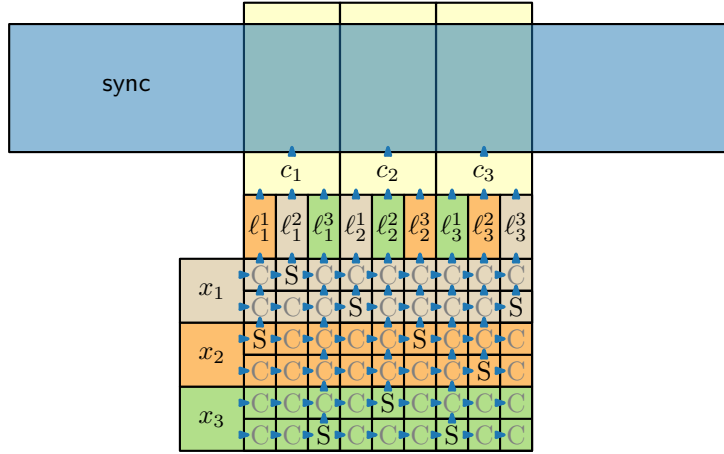


Figure 11: General grid structure used in our NP-hardness reduction. Here, we use the formula $\Phi = c_1 \wedge c_2 \wedge c_3$, where $c_1 = (\ell_1^1 \vee \ell_1^2 \vee \ell_1^3) = (x_2 \vee x_1 \vee \neg x_3)$, $c_2 = (\ell_2^1 \vee \ell_2^2 \vee \ell_2^3) = (\neg x_1 \vee x_3 \vee x_2)$, and $c_3 = (\ell_3^1 \vee \ell_3^2 \vee \ell_3^3) = (\neg x_3 \vee \neg x_2 \vee \neg x_1)$. There are variable gadgets (left), clause and literal gadgets (top), split gadgets (S), crossing gadgets (C), and a synchronization gadget (sync) spanning over all clause gadgets (blue rectangle). The gadgets have various states and orientations. The blue arrows mark in which direction the truth state of a satisfied literal *can* be propagated. The colors in the rows, i.e., brown, orange, green, correspond to the three variables x_1 , x_2 , and x_3 , respectively. The literal gadgets above have the same colors as the corresponding variables.

gadget. Each literal gadget and each clause gadget is in one of the states true or false. All clause gadgets are joined by a *synchronization gadget*. Within the column of each literal, we have a *split gadget* in one of the two rows of the corresponding variable x_i —in the upper row if the literal is x_i , and in the lower row if the literal is $\neg x_i$. In all other grid cells, we have *crossing gadgets*. Each of the split and crossing gadgets has four possible states, which we express in terms of both a horizontal orientation (left/right) *and* a vertical orientation (bottom/top), i.e., such a gadget can be oriented right and top, right and bottom, left and top, or left and bottom.

The general idea behind the construction is as follows: the initial drawing Γ and the final drawing Γ' differ only in the synchronization gadget; the rest of the construction is identical. Transforming the synchronization gadget from its initial to its final state is possible if and only if all clause gadgets are in their true state at the same time – both in Γ and Γ' all clause gadgets are however in their false state. A clause gadget can be in (or transformed into) its true state if and only if at least one of its three literal gadgets is in its true state – just like the clause gadgets, both in Γ and Γ' all literal gadgets are in their false state. A literal gadget can be in (or transformed into) its true state if and only if the state of the gadget of the variable of the literal is set accordingly (to true in case of positive literals and to false in case of negative literals). Both in Γ and Γ' , the state of all variable gadgets is unset, but they can be morphed easily (and independent of each other) to achieve any of their other two states. However, since a variable gadget is not directly joined with all of its literal gadgets, the state of the variable gadget needs to be propagated to the correct literal gadgets. To this end, we use crossing and split gadgets, which we discuss in the following paragraph.

A crossing or split gadget α can have the right horizontal orientation if and only if (1) the literal corresponding to its row is satisfied and (2) all gadgets strictly between α and the variable gadget in this row also have the right horizontal orientation – intuitively, the information that the literal is satisfied is transported from the variable gadget in a rightwards direction to α (and all gadgets in between). If these conditions are satisfied and α is a split gadget, then α can also have the top vertical orientation. The vertical orientation works similar to the horizontal orientation; a crossing or split gadget α that is located above the split gadget s of its column can have the top vertical orientation if and only if (1) s has the top vertical orientation, and (2) all gadgets in the column strictly between α and s have the top vertical orientation. Intuitively, the split gadget needs to receive the information that the literal in its row is satisfied via its horizontal orientation in order to propagate this information in the upwards direction to α (and all gadgets in between). In particular, a split or crossing gadget that is directly below a literal gadget can have the vertical orientation top if and only if the literal corresponding to the literal gadget is satisfied.

In summary, we can morph from Γ to Γ' if and only if we can transform the synchronization gadget, which is possible if and only if all clause gadgets are in the true state at the same time, which is possible if and only if at least

one literal gadget of each clause gadget is in the true state at the same time, which due to the propagation mechanism is possible if and only if the variables gadgets represent a satisfying truth assignment at the same time. (Notably, once the synchronization gadget has been transformed, it can remain in its altered state even if the other gadgets are morphed back to their states in Γ and Γ').

We proceed by discussing the low-level details of our construction.

Forbidden areas. In each gadget, we have *forbidden* areas where the vertices and edges cannot be drawn (henceforth drawn solid red). They are used to create a system of tunnels and cavities in which the edges of our drawings are placed and move; see, e.g., Fig. 17. We achieve this by populating the forbidden areas with obstacles, arranged on a fine grid (as explained in more detail in the paragraph “Running time” on page 20).

Variable gadget. The variable gadget has a comparatively simple structure; see Fig. 12. It has three vertices enclosed in a straight vertical tunnel of the forbidden area with one exit on the top right and one exit on the bottom right. Since the tunnel is straight, the middle vertex d , which we call *decision vertex*, is free (see Section 1 for the definition of free and see the thick blue–white vertex x_3 in Fig. 17 for the position of a free vertex in Γ and Γ'). We say that the variable gadget is in the state true (false) if d is moved to the top (bottom) position, and it is in the state unset otherwise. Consequently, we can move the top (bottom) vertex out of the vertical tunnel if and only if we are in the state true (false). We call a vertex that can be moved from its original position within a gadget into an adjacent gadget a *transferable* vertex. In the case of a variable gadget, one of the (black) neighboring vertices of d becomes a transferable vertex if the variable gadget is in the state true or false (see Figs. 12b and 12c).

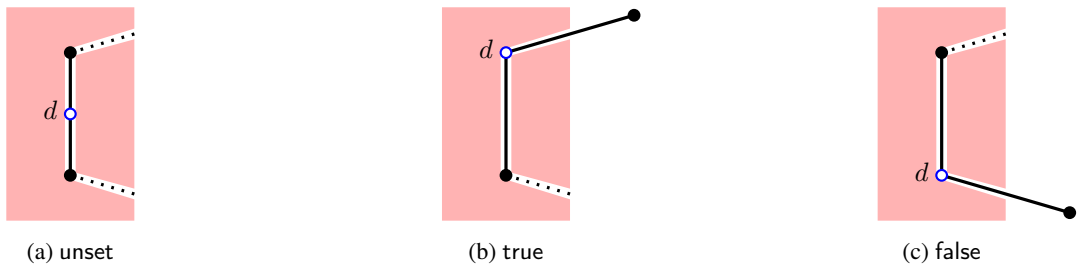


Figure 12: Variable gadget (a) in the state unset as it appears in Γ and Γ' , (b) in the state true, (c) in the state false.

Split gadget. A split gadget consists of a central vertex c of degree 3 together with paths to the left, right, and top; see Fig. 13. They are enclosed in a system of tunnels formed by the forbidden area. Fig. 13a shows a split gadget σ as it appears in Γ and Γ' . If the crossing/split/variable gadget to the left of σ , which shares the vertex l with σ , has a transferable vertex, then l can be moved to the next corner of the tunnel. Then, in turn, c can be moved to the bottom right corner of the white (obstacle-free) triangle in σ (see Fig. 13b), and the two other neighbors of c can be pushed one position to the right and one position up, allowing their neighbors (i.e., the (orange) vertices o and o' , respectively) to move to the next corner of the tunnel. In this case we say that the horizontal (vertical) orientation of σ is right (top) since o (o') is moved into the gadget to the top (right) of σ . The vertex o (o') becomes a transferable vertex.

Otherwise, the horizontal (vertical) orientation of σ is left (bottom). This corresponds to *not* forwarding the value true to the gadget on the right (top).

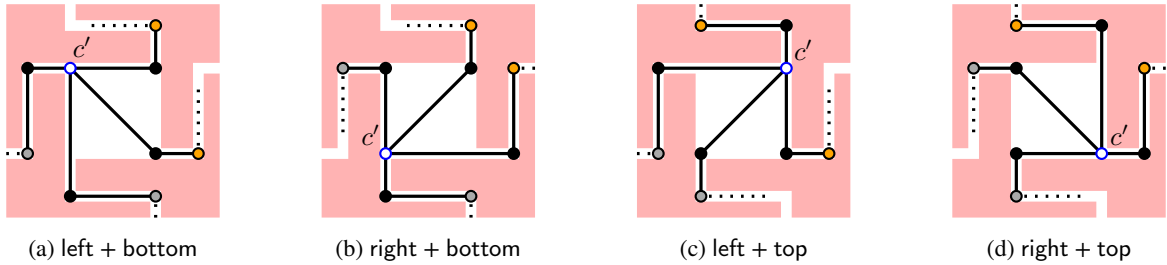
Crossing gadget. A crossing gadget has a similar structure as a split gadget. However, we now have a central vertex c' of degree 4 with paths to the neighboring gadgets to the left, right, top, and bottom. In the center of the crossing gadget χ in Fig. 14, there is a white (obstacle-free) square. In Γ and Γ' , c' is placed in the top left corner of this square (see Fig. 14a). If the gadget on the left of χ has a transferable vertex, we can push the adjacent vertices to the next corners of the tunnel such that c' can move to the bottom side of the square (see Figs. 14b and 14d). Only then can we push the vertices of the path leaving the gadget on the right side to the next corner of the tunnel. In this case, we have a transferable vertex, and we say that the horizontal orientation of the crossing gadget is right; otherwise it is left. Symmetrically, if the gadget below χ has a transferable vertex, we can move c' to the right side of the square (see Figs. 14c and 14d). Only then can we push the vertices of the path leaving χ through the top side to the next corner of the tunnel. In this case we have a transferable vertex and we say that the vertical orientation of the crossing gadget



(a) Split gadget as it appears in Γ and Γ' with horizontal and vertical orientation left and bottom.

(b) If the gadget on the left has horizontal orientation right, vertices can be pushed one position further and we can reach the orientations right and top.

Figure 13: Split gadget: from a horizontal row transporting a truth value, we “copy” the same truth value up to a vertical column.



(a) left + bottom

(b) right + bottom

(c) left + top

(d) right + top

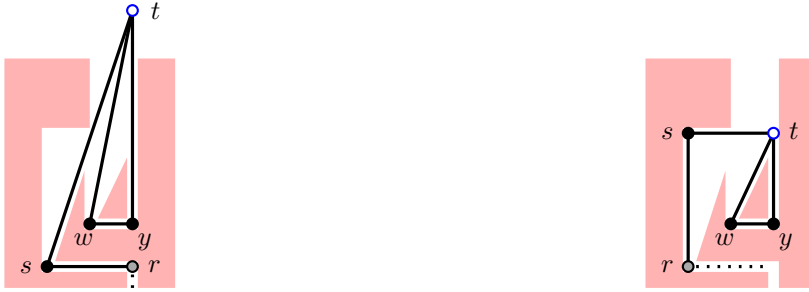
Figure 14: Crossing gadget: we transport truth values horizontally and vertically without influencing each other. The four possible combinations of orientations are illustrated.

is top; otherwise it is bottom. Observe that the states of the gadgets on the left and below χ *independently* determine the horizontal and vertical orientation of χ . This property assures that we can transport information along routes that cross each other, but do not influence each other. We remark that not all crossing gadgets transmit information both to the right and to the top. If a crossing gadget is directly below a split gadget, then no information is pushed from the crossing to the split gadget as no vertex can be moved into a split gadget from below. The blue arrows in Fig. 11 indicate where information is pushed and where it is not. Figure 17 shows in more detail that there is no connection between a split gadget and the crossing gadget below. In such a case, the positions of the vertices in the crossing gadget that would lead to the gadget above are irrelevant for our reduction.

Literal gadget. Fig. 15 shows a literal gadget λ as it appears in Γ and Γ' . It consists of five vertices, one of which, r , is shared with the gadget β below; see Fig. 15. Only if the vertical orientation of β is top, vertex r can move to the original position of s and s can move up. This in turn allows vertex t to move into the interior of λ . In this case, we say that λ has the state true; otherwise, it has the state false. If a cycle in Γ or Γ' contains obstacles, we call the cycle an *anchor*. Observe that the anchor $\langle t, w, y \rangle$ restricts the area where we can move t .

Clause gadget. Each clause c_i ($i \in [m]$) is represented by a clause gadget, which consists of a path of length 9 whose endpoints are anchored by two 3-cycles; see Fig. 16. In the clause gadget as it appears in Γ and Γ' (see Fig. 16a), we have exactly one free vertex (denoted by y , or, to indicate that it belongs to clause c_i , denoted by y_i), which is at the bottom of a large rectangular obstacle-free region, which is also part of the synchronization gadget. Observe that, within this area, we cannot move y (up to a tiny bit) to the left or right due to its neighbors lying at (essentially) fixed positions (see Fig. 16a).

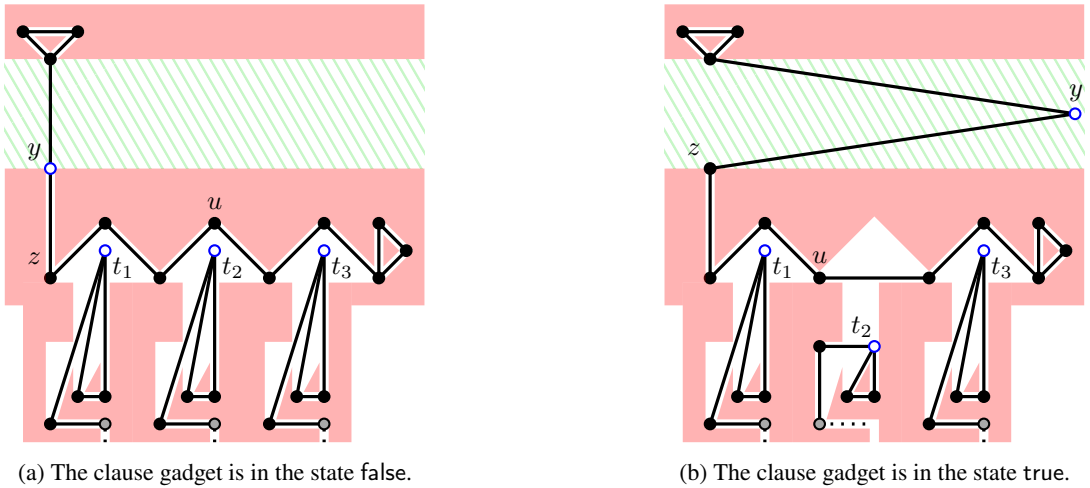
However, if one of the incident literal gadgets is in the state true, we can get a second free vertex by moving it onto the straight-line segment defined by its two neighbors (in Fig. 16a, that vertex is called u). Then, we can push, starting at that second free vertex (i.e., u in Fig. 16), each vertex by one position to its successor until we have pushed z to the position where y is located in Γ and Γ' (see Fig. 16b). Now y becomes a transferable vertex (we assume that we push y out of the clause gadget into the synchronization gadget). We can move y arbitrarily far to the right within this obstacle-free region (unless y is blocked by the edges of another clause gadget). Only when this is done for all clause



(a) State false where vertex t is above the forbidden area of the gadget. This is the literal gadget as it appears in Γ and Γ' .

(b) State true where vertex t is inside the cavity formed by the forbidden area of the gadget. This state can only be reached if the split or crossing gadget below has orientation top.

Figure 15: Literal gadget: Depending on the crossing or split gadget below, it can be in two different states. Only in the state true, vertex t does not pop out of the gadget.



(a) The clause gadget is in the state false.

(b) The clause gadget is in the state true.

Figure 16: Clause gadget together with three literal gadgets: If at least one of the literal gadgets is in the state true, the clause gadget is also in the state true. The obstacle-free region shared with the synchronization gadget is depicted in hatched green.

gadgets simultaneously, the synchronization gadget (see below) can be morphed as desired. Thus, we say that a clause gadget is in the state true if at least one of its literal gadgets is in the state true; otherwise it is in the state false.

Synchronization gadget. The synchronization gadget is a 3-cycle $\langle v_1, v_2, v_3 \rangle$; see Fig. 17.

In Γ , this cycle is drawn as a isosceles triangle T with base v_2v_3 that has v_1v_2 as a vertical edge and with v_3 to the left of this edge (the exact shape or size of T is not relevant). In Γ' , this cycle is drawn as a shifted version (see Section 1 for the definition) of T , which we call T' . Apart from this, Γ and Γ' are identical. The drawing T is blocked from T' due to Proposition 8 (we use the same construction as in the proof): inside of T , we have obstacles $a', b',$ and c' arranged with ε distance next to $v_1, v_2,$ and v_3 , respectively. Outside of T and with ε distance to the midpoint of the edge v_1v_3 , we have an obstacle d' . According to Proposition 8, it suffices to set ε to some constant at most $s/12$ where s is the length of the edge v_2v_3 in Γ . The only difference to the construction in Proposition 8 is that we do not have an obstacle e' , but we emulate the functionality of e' by edges of the clause gadgets: T and the obstacles $a', b', c',$ and d' are located in the large rectangular obstacle-free region of the clause gadget such that v_1v_2 lies directly to the left of the edge of the clause gadget that has y_1 as its lower endpoint (initially). We scale the rest of our construction such that the midpoint of the edge v_1v_2 is within ε distance to all the edges of the clause gadget that have one of the

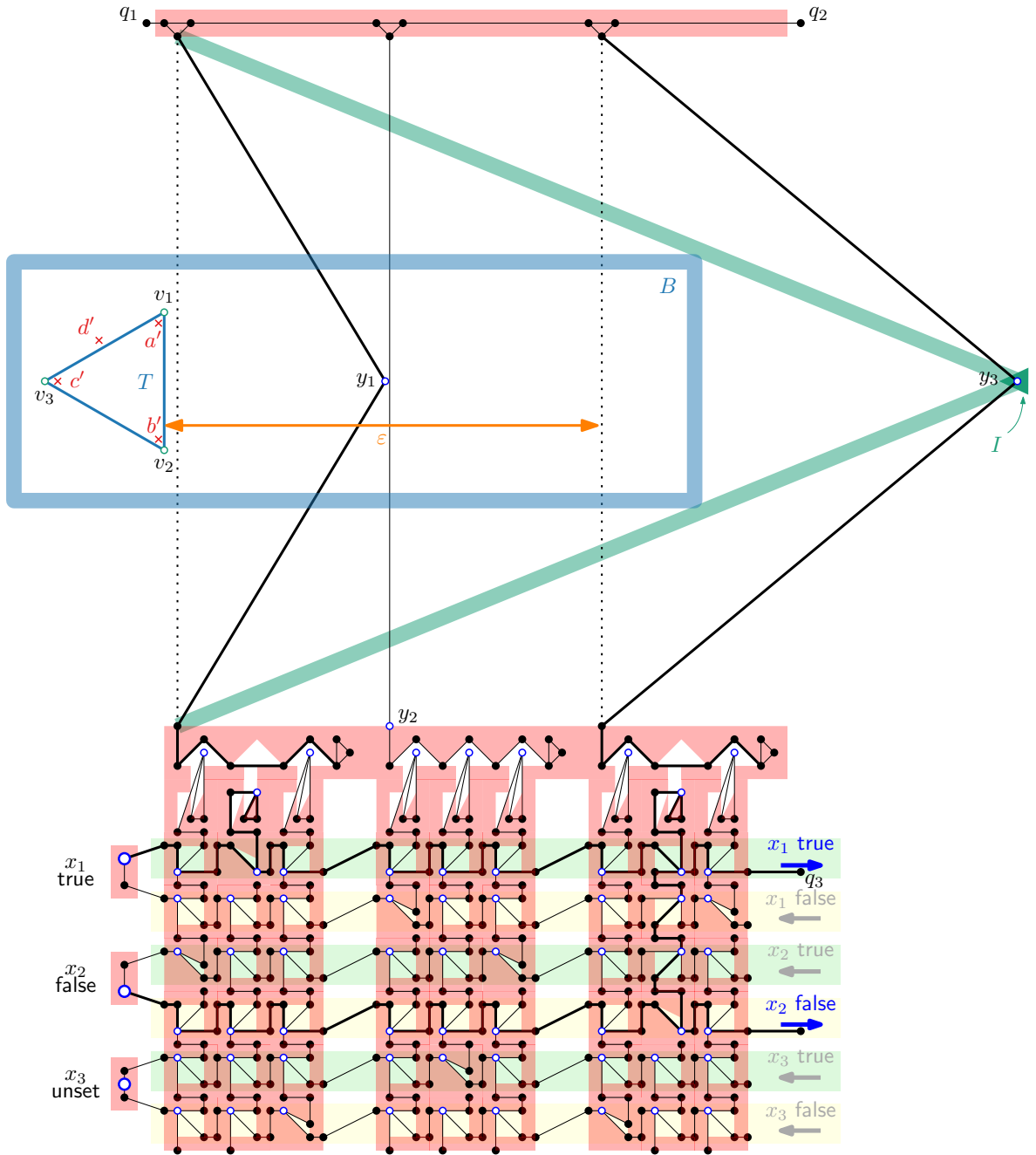


Figure 17: Full construction for $\Phi = (x_2 \vee x_1 \vee \neg x_3) \wedge (\neg x_1 \vee x_3 \vee x_2) \wedge (\neg x_3 \vee \neg x_2 \vee \neg x_1)$. Gadgets with orientation right/top/true use thicker strokes. The triangle T and the height of the clause gadgets is scaled down; the rest is scaled up. The blue box B indicates the free area where T can rotate. The green bars and I indicate how the edges incident to y must bend to leave B empty. The green and yellow horizontal strips contain the gadgets of the unnegated and negated literals, respectively.

vertices y_i as their lower endpoint (initially).³ We emphasize that (the coordinates of) T , the obstacles a', b', c', d' , and the distance ε do not depend on Φ (i.e., we can use the same T, a', b', c', d' for every given Boolean formula Φ).

³Note that even if a clause gadget is in the state false, we have a little flexibility in morphing the edges incident to y due to the width of the tunnel in which the edge yz lies. When scaling the construction to have the edges incident to y in ε distance to the midpoint of $v_1 v_2$, we account for this little extra slack.

Hence, we can hard-code them into our reduction algorithm (the size of their encodings is constant); cf. Proposition 8. By Proposition 5, there exists an obstacle-avoiding planar morph M from T to T' with respect to the obstacle set formed by only the four obstacles a' , b' , c' , and d' . Let B be an axis-aligned rectangle (or bounding box) that contains all drawings of M in its interior. The height of the large rectangular obstacle-free region of the synchronization gadget is chosen such that the region contains B . Given that T , T' , a' , b' , c' , and d' do not depend on Φ , it follows that M , and B also do not depend on Φ . Thus, the positions of the corners of B have constant-sized coordinates, which can again be hard-coded into our reduction algorithm.

Correctness. We first show a key property of the synchronization gadget. If Γ can be morphed such that no edge or vertex except for T lies inside B , then T can be morphed to the shifted version T' , and, after that, the first step of morphing Γ can be reversed so that the final drawing coincides with Γ' . Due to the placement of T , a' , b' , c' , and d' , this is possible if and only if all of the clause gadgets are in the state true: in this case, for each clause c_i , we can move the vertex y_i in the clause gadget of c_i into a region I on the far right side so that the edges incident to y_i do not intersect B . In contrast, if a clause gadget is in the state false, at least one of the edges incident to its vertex y_i contains a point of distance at most ε to the midpoint of v_1v_2 , which means that we cannot morph T to T' by Proposition 8.

Now, if Φ admits a satisfying truth assignment, we can describe a morph from Γ to Γ' by moving the decision vertices in the variable gadgets according to the truth assignment, which allows to transport these truth values via the split and crossing gadgets to the literal and the clause gadgets. As all clause gadgets can reach the state true at the same time, we can morph the drawing of the 3-cycle in the synchronization gadget to its shifted version and then move all other vertices back to their original position. (Note that this morph can also be turned into a piecewise linear one by Observation 2.)

For the other direction, if a morph from Γ to Γ' exists, then we know by our construction that at some point, all clause gadgets were in the state true simultaneously (as this is necessary to morph the drawing of the 3-cycle in the synchronization gadget to its shifted version), which means the variable gadgets represent at the same time a satisfying truth assignment for Φ .

Running time. As stated above, we realize the forbidden areas in our gadgets by populating them with obstacles placed on a fine grid. For each gadget type \mathcal{T} other than the synchronization gadget, there clearly exists a grid that is fine enough to ensure the desired functionality of the gadget. Essentially the required resolution of the grid is a function in the width of the tunnels used in \mathcal{T} . Notably, the design of \mathcal{T} (in particular, the width of the tunnels and, thus, the resolution) does not depend on Φ . Hence, the number of obstacles used in \mathcal{T} is $O(1)$ and there is a constant-time algorithmic subroutine that creates \mathcal{T} at some fixed location in the plane (for each gadget type \mathcal{T}). By extension, there exists a polynomial-time algorithm (note that the overall number of used gadgets is $O(nm)$) that creates the desired grid-like arrangement of translated copies of gadgets that make up the *bottom part* (everything below the synchronization gadget) of our construction. Regarding the synchronization gadget, recall that the coordinates of the vertices of T and the obstacles a' , b' , c' , and d' , as well as the distance ε and the corners of B also do not depend on Φ and can, thus, be hard-coded (determined in constant time) into the reduction algorithm. To the right side of the triangle T , we slice a vertical strip of (constant) width ε into m vertical substrips—one for each clause gadget. The bottom part of our construction is now scaled as stated in the description of the synchronization gadget, which decreases the the width and height of each gadget in the bottom part to $\Theta(1/m)$, which can again be done in polynomial time (recalling that the number of gadgets is $O(nm)$).

Connectivity. So far, the graph in our reduction has $\Omega(m)$ connected components: a large connected component comprising all variable, split, crossing and literal gadgets, a connected component for all clause gadgets, as well as another connected component for the synchronization gadget. We can merge these components by adding edges without influencing the behavior of our gadgets; see Fig. 17: We can add a constant-length path between the vertices labeled v_1 and q_1 (this leaves sufficiently much freedom for T to morph to T') and another constant-length path between the vertices labeled q_2 and q_3 (near the upper blue arrow in Fig. 17). \square

Remark 1 (Bounded number of obstacles per face). In our NP-hardness construction, even after connecting the graph, there are faces containing a large number of obstacles. Now one might wonder whether the problem becomes easier if we have a small constant number of obstacles per face. However, this is not the case because in a slightly adjusted NP-hardness construction, every face has at most one obstacle: enclose every obstacle of the current construction by a separate 3-cycle and connect this 3-cycle via a sufficiently long path to one of the vertices of the

considered face. Now, clearly, every face has at most one obstacle and these new parts do not restrict the functionality of the gadgets because we have added them via sufficiently long paths.

6. Open Problems

1. In general, the decision problem whether, for two crossing-free straight-line drawings of the same graph, there exists an obstacle-avoiding crossing-free morph is NP-hard (Theorem 1). However, it can be solved efficiently for forests (Proposition 3). Are there other meaningful graph classes where this is the case? In particular, what about cycles or triangulations? It is conceivable that the latter case is actually easier since the placement of obstacles that are compatible with the two given drawings is quite limited. Regarding cycles, we emphasize that the existence of a free vertex is not a sufficient condition for the existence of a morph (cf. Fig. 3).
2. Does the problem lie in NP? Is it $\exists\mathbb{R}$ -hard?
3. Our NP-hardness reduction in the proof of Theorem 1 uses a large number of obstacles. On the other hand, Proposition 4 says that every plane graph admits an obstacle-avoiding morph from one drawing to another if the number of obstacles (compatible with the two drawings) is at most 2. So for how many obstacles does the problem become NP-hard?
4. The drawings Γ and Γ' produced by our reduction are identical except for the position of three vertices. Does the problem become easier when only up to two vertices may change positions?
5. It is easy to observe that if our reduction is applied to a satisfiable formula Φ with n variables and m clauses, there is a piecewise linear planar obstacle-avoiding morph between the produced drawings Γ and Γ' with $\Theta(n + m)$ steps, which is also necessary. Note that this number depends on the size of the output of the reduction. This motivates the following family of questions. Let k be an arbitrary fixed constant. Given two planar straight-line drawings Γ and Γ' of the same plane graph and a set of obstacles compatible with Γ and Γ' , decide whether there exists a piecewise linear planar obstacle-avoiding morph from Γ to Γ' with at most k steps. For which values of k can this decision problem be answered efficiently?
6. Given two drawings of the same plane graph, how many compatible obstacles are necessary and sufficient to block them? Can this be computed efficiently?
7. Lubiw and Petrick [17] studied the problem of morphing drawings of graphs where edges can be drawn as polygonal chains, that is, edges are allowed to bend. Does morphing in the presence of obstacles remain NP-hard if we allow a certain (say, constant) number of bends per edge? This can be seen as a special case of our problem where the input is restricted to graphs whose edges have been subdivided a certain number of times.

References

- [1] Oswin Aichholzer, Greg Aloupis, Erik D. Demaine, Martin L. Demaine, Vida Dujmović, Ferran Hurtado, Anna Lubiw, Günter Rote, André Schulz, Diane L Souvaine, and Andrew Winslow. Convexifying polygons without losing visibilities. In Greg Aloupis and David Bremner, editors, *CCCG*, pages 229–234, 2011. URL: <http://www.cccg.ca/proceedings/2011/papers/paper70.pdf>.
- [2] Soroush Alamdari, Patrizio Angelini, Fidel Barrera-Cruz, Timothy M. Chan, Giordano Da Lozzo, Giuseppe Di Battista, Fabrizio Frati, Penny Haxell, Anna Lubiw, Maurizio Patrignani, Vincenzo Roselli, Sahil Singla, and Bryan T. Wilkinson. How to morph planar graph drawings. *SIAM J. Comput.*, 46(2):824–852, 2017. doi:10.1137/16M1069171.
- [3] Helmut Alt, Christian Knauer, Günter Rote, and Sue Whitesides. On the complexity of the linkage reconfiguration problem. In *Towards a Theory of Geometric Graphs*, volume 342 of *Contemporary Mathematics*, pages 1–14. American Mathematical Society, Providence, 2004.
- [4] Patrizio Angelini, Giordano Da Lozzo, Fabrizio Frati, Anna Lubiw, Maurizio Patrignani, and Vincenzo Roselli. Optimal morphs of convex drawings. In Lars Arge and János Pach, editors, *SoCG*, volume 34 of *LIPICs*, pages 126–140. Schloss Dagstuhl – Leibniz-Zentrum für Informatik, 2015. doi:10.4230/LIPICs.SOCG.2015.126.
- [5] Elena Arseneva, Prosenjit Bose, Pilar Cano, Anthony D’Angelo, Vida Dujmović, Fabrizio Frati, Stefan Langerman, and Alessandra Tappini. Pole dancing: 3D morphs for tree drawings. *J. Graph Algorithms Appl.*, 23(3):579–602, 2019. doi:10.7155/jgaa.00503.
- [6] Elena Arseneva, Rahul Gangopadhyay, and Aleksandra Istomina. Morphing tree drawings in a small 3D grid. *J. Graph Algorithms Appl.*, 27(4):241–279, 2023. doi:10.7155/jgaa.00623.
- [7] Kevin Buchin, Will Evans, Fabrizio Frati, Irina Kostitsyna, Maarten Löffler, Tim Ophelders, and Alexander Wolff. Morphing planar graph drawings through 3D. *Comput. Geom. Topol.*, 2(1):5:1–5:18, 2023. doi:10.57717/cgt.v2i1.33.
- [8] Stewart S. Cairns. Deformations of plane rectilinear complexes. *Amer. Math. Monthly*, 51(5):247–252, 1944. doi:10.1080/00029890.1944.11999082.

- [9] Éric Colin de Verdière and Arnaud de Mesmay. Testing graph isotopy on surfaces. *Discret. Comput. Geom.*, 51(1):171–206, 2014. doi:10.1007/s00454-013-9555-4.
- [10] Robert Connelly, Erik D. Demaine, Martin L. Demaine, Sándor P. Fekete, Stefan Langerman, Joseph S. B. Mitchell, Ares Ribó, and Günter Rote. Locked and unlocked chains of planar shapes. *Discrete Comput. Geom.*, 44(2):439–462, 2010. doi:10.1007/s00454-010-9253-3.
- [11] Robert Connelly, Erik D. Demaine, and Günter Rote. Straightening polygonal arcs and convexifying polygonal cycles. *Discrete Comput. Geom.*, 30:205–239, 2003. doi:10.1007/s00454-003-0006-7.
- [12] Giordano Da Lozzo, Giuseppe Di Battista, Fabrizio Frati, Maurizio Patrignani, and Vincenzo Roselli. Upward planar morphs. *Algorithmica*, 82(10):2985–3017, 2020. doi:10.1007/s00453-020-00714-6.
- [13] Oksana Firman, Tim Hegemann, Boris Klemz, Felix Klesen, Marie Diana Sieper, Alexander Wolff, and Johannes Zink. Morphing graph drawings in the presence of point obstacles. In Henning Fernau, Serge Gaspers, and Ralf Klasing, editors, *SOFSEM*, volume 14519 of *LNCS*, pages 240–254. Springer, 2024. doi:10.1007/978-3-031-52113-3_17.
- [14] Jonas Gomes, Lucia Darsa, Bruno Costa, and Luiz Velho. *Warping and Morphing of Graphical Objects*. Morgan Kaufmann, 1999.
- [15] Linda Kleist, Boris Klemz, Anna Lubiw, Lena Schlipf, Frank Staals, and Darren Strash. Convexity-increasing morphs of planar graphs. *Comput. Geom.*, 84:69–88, 2019. doi:10.1016/j.comgeo.2019.07.007.
- [16] Boris Klemz. Convex drawings of hierarchical graphs in linear time, with applications to planar graph morphing. In Petra Mutzel, Rasmus Pagh, and Grzegorz Herman, editors, *ESA*, volume 204 of *LIPICs*, pages 57:1–57:15. Schloss Dagstuhl – Leibniz-Zentrum für Informatik, 2021. doi:10.4230/LIPICs.ESA.2021.57.
- [17] Anna Lubiw and Mark Petrick. Morphing planar graph drawings with bent edges. *J. Graph Algorithms Appl.*, 15(2):205–227, 2011. doi:10.7155/jgaa.00223.
- [18] Helen C. Purchase, Eve E. Hoggan, and Carsten Görg. How important is the “mental map”? – An empirical investigation of a dynamic graph layout algorithm. In Michael Kaufmann and Dorothea Wagner, editors, *GD*, volume 4372 of *LNCS*, pages 184–195. Springer, 2006. doi:10.1007/978-3-540-70904-6_19.
- [19] Carsten Thomassen. Deformations of plane graphs. *J. Combin. Theory Ser. B*, 34(3):244–257, 1983. doi:10.1016/0095-8956(83)90038-2.